Solid State Phenomena
ISSN: 1662-9779, Vol. 360, pp 151-155
doi:10.4028/p-BgTrK1

Submitted: 2023-09-08
Revised: 2023-09-30
Accepted: 2024-03-08
Online: 2024-08-23

Experimental Demonstration and Analysis of 3.3kV 4H-SiC Common-Drain Bidirectional Charge-Balanced Power MOSFETs

Mohamed Torky[1,a*], Zhaowen He[1,b], Collin Hitchcock[2,c], Reza Ghandi[2,d], Stacey Kennerly[2,e] and T. Paul Chow[1,f]

[1]Rensselaer Polytechnic Institute, 110 8th Street, Troy, New York 12180, U.S.A

[2]GE Global Research, 1 Research Circle, Niskayuna, New York 12309, U.S.A.

[a]torkym@rpi.edu, [b]hez5@rpi.edu, [c]collin.hitchcock@ge.com, [d]ghandi@ge.com, [e]Stacey.kennerly@ge.com , [f]chowt@rpi.edu

Keywords: Bidirectional 4H-SiC MOSFET, 4H-SiC Charge-Balanced MOSFET,

Abstract. By using 4H-SiC packaged Charge-Balanced (CB) MOSFET, we have experimentally demonstrated a 3.3kV 4H-SiC common-drain bidirectional (BD) CB power MOSFET and measured its static and dynamic characteristics compared to its unidirectional counterpart. We show that the BD CB MOSFET conducts and blocks at the first and third quadrants with the appropriate gate bias with an on-state resistance double its unidirectional counterpart, while its switching energies are 12 (19) and 34 (12) mJ/cm^2 for BD CB MOSFET (UD CB MOSFET)

Introduction.

4H-SiC has superior material and electrical properties compared to Si such as 10x critical electric field, enabling high-voltage devices with a significant (~1000 times) reduction in on-state resistance. Also, the charge-balanced (CB) design concept for the drift region of unipolar power devices involves constructing a 3D network of buried p-type regions (CB-regions) surrounded by n-type regions with balanced doping concentrations to achieve a rectangular field profile enhancing the on-state resistance as shown in Figure 1c [1-2]. Bidirectional (BD) transistor switches are highly desirable for high voltage efficient power electronic circuits and applications such as Power Factor Corrector (PFC) rectifiers, matrix converters, and multilevel PV inverter [3-5], reducing system complexity, size, and cost. In this paper, we implemented and characterized a back-to-back (common drain), hybrid 3.3kV BD CB SiC power MOSFET, showing its static and dynamic performance. We adopt the back-to-back common-drain configuration as it is more physically feasible with the least number of semiconductor devices and with no parasitic lead resistance or inductance compared to other BD switch realizations [6], yet it introduces some circuit complexity, where the gates must have their own gate driver because they are referenced to their corresponding source terminal as depicted in Figure 1b [6]. For the common-drain configuration, the SiC BD CB DMOSFET cannot share the same pillars in the drift region because, in that case, the parasitic open base BJT cannot support high voltage. Accordingly, we implemented the hybrid configuration for 3.3kV BD CB SiC DMOSFETs and compared it with the 3.3kV unidirectional (UD) CB SiC DMOSFET as shown in Figure 1c and Figure 1d.

Methodology.

By using two packaged 3.3kV CB MOSFETs, we implemented the Hybrid-BD CB MOSFETs by adhering two-packaged devices back-to-back using NBE Technologies NanoTach-X nanosilver paste, which was then sintered to 150°C for 30 minutes. A photograph, circuit schematic and cross-section schematic of Hybrid-BD CB MOSFET is shown in Figure 1.

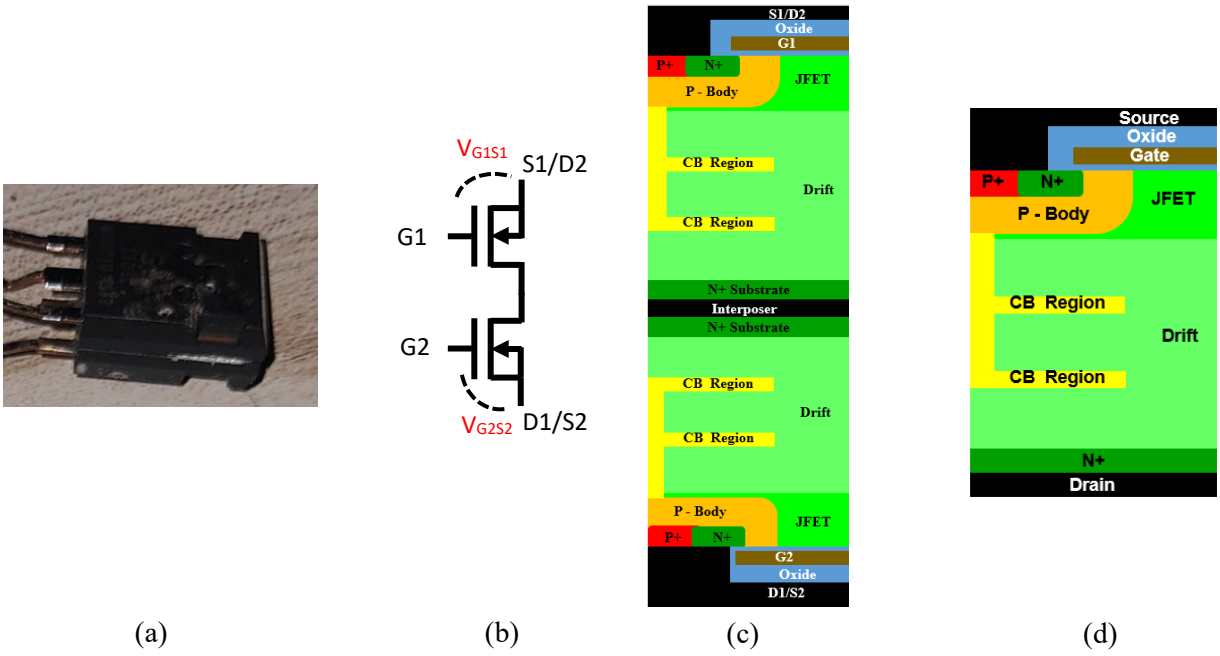

(a) (b) (c) (d)

Fig. 1. (a) Back-to-back hybrid bidirectional (Hybrid-BD) CB MOSFET, (b) the circuit schematic of Hybrid-BD CB MOSFET, (c) schematic half-cell cross-section of Hybrid-BD CB MOSFET, and (d) schematic half-cell cross-section of UD CB MOSFET

Both static and dynamic measurements are performed for Hybrid-BD CB and UD CB MOSFETs to evaluate and compare their performance. The conduction measurement has been taken using at different temperature levels (RT, 100 °C and 150 °C) by using Kelvin contact to eliminate the parasitic resistance of the wires. While the blocking static measurement has been taken with the ultra-high voltage (UHV) expander. For the dynamic characteristics, room temperature inductive switching measurements have been taken using a customized double pulse testing system. The power supply has been kept at 2kV and the gate pulse width has been chosen to ensure a 70A/cm^2 current density flows through the CB MOSFETs. Since the common-drain configuration needs two different gate drivers for each gate, only one device was switched, and the other device gate voltage was kept under 18V.

Results.

The output characteristics (shown in Figure 2) of Hybrid-BD CB DMOSFET shows a specific on-resistance of 18mΩ.cm^2 at 1.1A (100A/cm^2) which is twice the UD CB MOSFET. The increase of $R_{ON,sp}$ at 100°C and 150°C is 1.3x and 2x compared to $R_{ON,sp}$ at room temperature because the temperature dependence of the bulk mobility is given by a power law of $T^{-2.3}$, hence increasing the specific on-resistance at the drift, and JFET regions. Generally, $R_{ON,sp}$ increases faster at higher temperatures because the difference between the channel and bulk mobilities temperature dependence as the channel mobility has a weak temperature dependence. So, at higher temperatures, the drift and JFET specific on-resistances become more dominant than at lower temperatures.

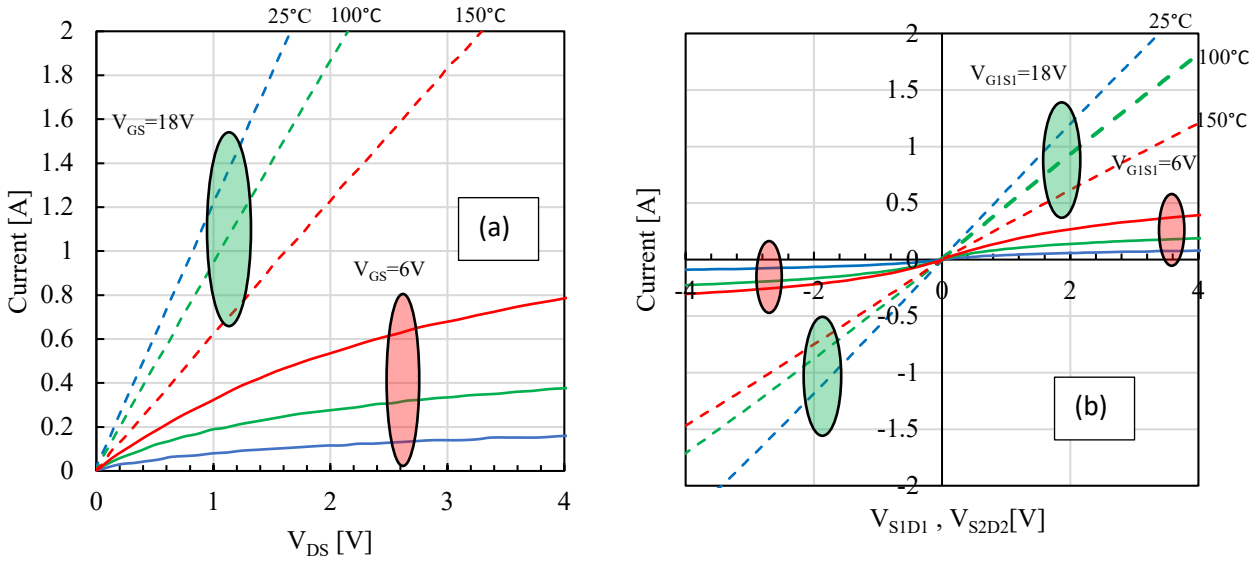

Fig. 2. Output characteristics of (a) unidirectional BD CB MOSFET and (b) Hybrid-BD CB MOSFET at different temperature.

For the blocking state as depicted in Figure 3, the device blocks symmetrically a voltage in the two directions of 3.6kV with a leakage current of 10µA. The drift region of the Hybrid-BD CB DMOSFET is not a sharing-drift region, consequently, the device with the low potential side blocks. That is why the gate of the high potential side can be kept at 18V relative to its source as it does not support the voltage.

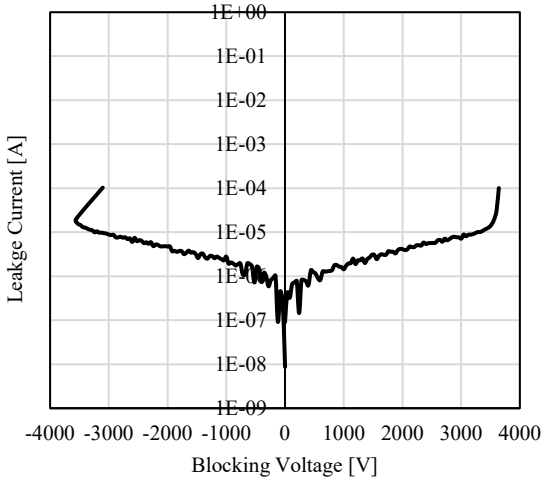

Fig. 3. Blocking characteristics for Hybrid-BD CB MOSFET

Compared to previously reported conventional MOSFETs as shown in Figure 4, CB MOSFET has a better trade-off compared to conventional MOSFETs due to the rectangular electric field profile. UD BD CB SiC MOSFET has a better $R_{ON,sp}$ reduction of at least 10% (up to 50%) compared to the best reported conventional SiC MOSFETs enhancing the conduction losses.

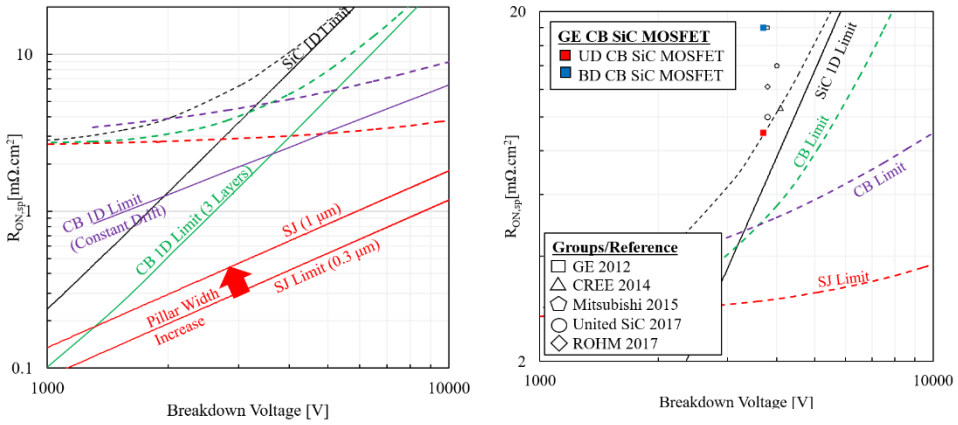

Fig. 4. $R_{ON,sp}$ vs. BV for 3.3kV SiC unidirectional and bidirectional CB MOSFET with other reported devices. Dashed lines include the channel and JFET regions.

A double-pulse inductive switching testing was performed for the BD (and UD) CB DMOSFET at 2kV and 70A/cm^2 as illustrated in Fig. 5 & 6. The specific switching energy losses per cycle with $E_{OFF,sp}$ and $E_{ON,sp}$ are 12 (19) and 34 (12) mJ/cm^2 respectively. CB MOSFETs offer a 50% lower conduction loss but at the expense of switching loss due to the high resistive RC network of P-bus and CB regions. The doubled specific switching energy in the on-cycle of the Hybrid-BD CB MOSFET is since only one device is blocking, so when the device is switching from off to on states, the two devices are responsible for the conduction. In contrast, at the switching off, one device will eventually block the voltage. At low-frequency applications where conduction losses dominate, CB MOSFETs remain advantageous.

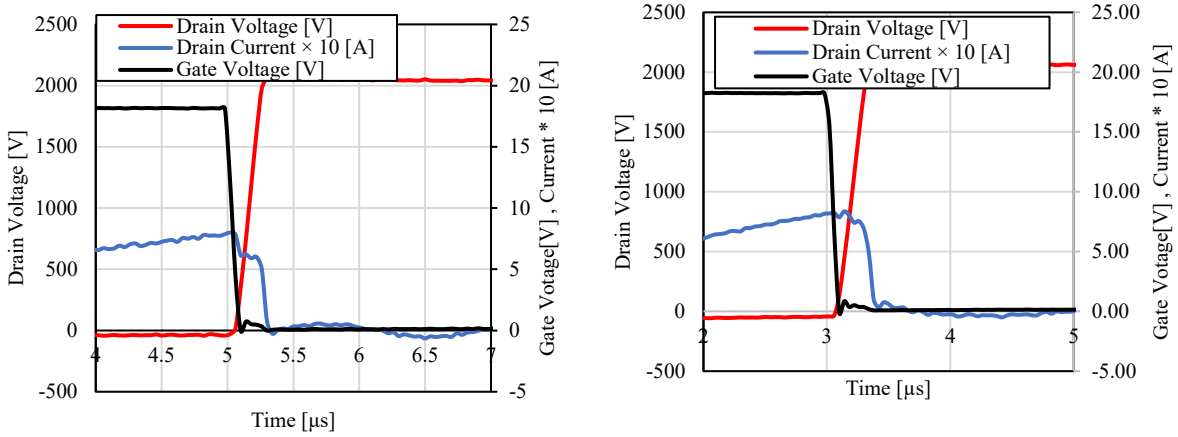

Fig. 5. Turn-on waveforms of (a) Hyrbid-BD CB MOSFET and (b) UD CB MOSFET

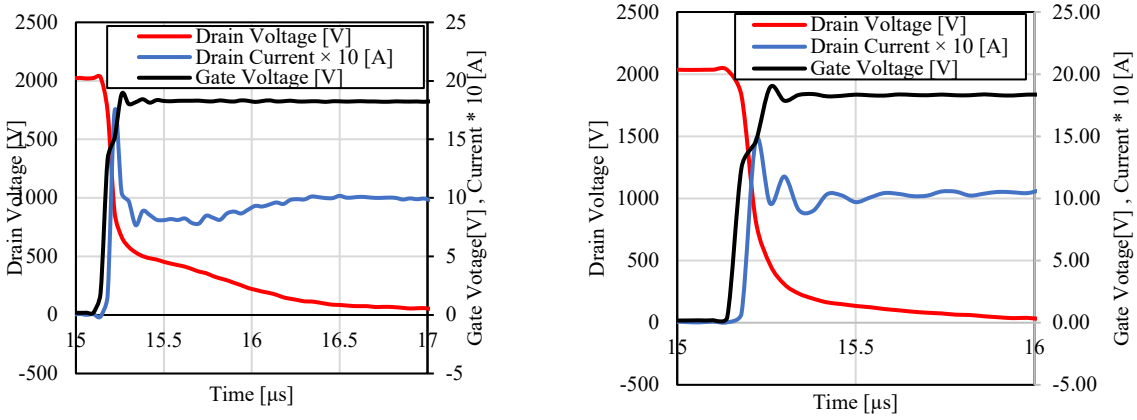

Fig. 6. Turn-off waveforms of (a) Hyrbid-BD CB MOSFET and (b) UD CB MOSFET

Conclusion

We have implemented a 3.3kV Hybrid-BD CB MOSFET by connecting two CB MOSFET from GE in a package form. We compared the static and dynamic characteristics of Hybrid-BD and UD CB MOSFETs at different temperatures showing that the on-state resistance of the Hybrid-BD CB MOSFFET is double that of its UD counterpart. We also showed that the newly demonstrated BD MOSFET has AC switch characteristics where it conducts and blocks in both directions. We also measured the dynamic characteristics of both devices illustrating the energy losses between the BD and UD devices.

References

[1] A. Bolotnikov, P. Losee, S. Kennerly, R. Datta, and X. She, ICSCRM, (2018).

[2] R. Ghandi, A. Bolotnikov, D. Lilieneld, S. Kennerly, R. Ravisekhar, Proc. ISPSD, p.179, (2019).

[3] T. B. Soeiro, T. Friedli and J. W. Kolar, Soeiro, Twenty-Seventh Annual IEEE Applied Power Electronics Conference and Exposition (APEC), 2617 (2012).

[4] S.K. Kuncham, K. Annamala, S. Nallamothu, International Journal of Circuit Theory and Applications, vol. 47, p. 152 2019.

[5] P. W. Wheeler, J. Rodriguez, J. C. Clare, L. Empringham and A. Weinstein, IEEE Transactions on Industrial Electronics, vol. 49, p. 276, (2002).

[6] C. Hitchcock and T. Paul Chow, Mat. Sci. Forum, (2020).

[7] H. Naik, K. Tang, T. Marron, T. P. Chow, and J. Fronhesier, Mater. Sci. Forum, vol. 615, p.785, (2009).

[8] A. Bolotnikov et al., Proc. ISPSD, p.389, (2012).